Engineering Research Journal
journal homepage: https://erj.journals.ekb.eg/

Experimental Investigation on The Compressive Behaviour of GFRP-Reinforced Concrete Short Columns

Shawki A. Emam[1], Osama Amer[2,*], Ahmed H. Ali[1], Hisham Haggag[1]

[1] Department of Civil Engineering, Faculty of Engineering Mataria, Helwan University, Cairo, Egypt

[2] Department of Civil Engineering, Ain Shams University, Cairo, Egypt

[*]Corresponding author E-mail: osama_amer@cu.edu.eg, Osama_oo@yahoo.com

Abstract. This study investigates the compressive response of concrete columns incorporating Glass Fiber-Reinforced Polymer (GFRP) reinforcement bars under eccentric vertical loading conditions. The experimental study encompassed six reinforced concrete (RC) columns, partitioned into two groups: one incorporating conventional reinforcement steel and the other utilizing GFRP longitudinal reinforcement bars. The primary variables considered included reinforcement type, reinforcement ratio, and eccentricity-to-thickness (e/t) ratio. The objective was to evaluate the structural performance of GFRP bars as primary reinforcement in RC columns and assess their viability as a substitute for steel reinforcement in compression-dominated applications. The results revealed pronounced disparities in load-carrying capacities and ductility, particularly under varying e/t ratios, underscoring the significance of reinforcement material on column response. These findings promote to the advancement of knowledge on the performance characteristics of GFRP-reinforced concrete columns and provide essential insights for their implementation in structural design.

Keywords: GFRP bars, Reinforced concrete, RC columns, Eccentric loading, Load-displacement behaviour, Failure modes, Ductility, Structural performance.

1 Introduction

The durability of RC structures remains a critical issue within the building and construction field, with corrosion of steel reinforcement being a primary contributor to the degradation and compromised structural integrity of such systems. This ubiquitous phenomenon manifests in diverse environments, including coastalregions [1], areas subjected to frequent applications of de-icing salts [2], and industrial facilities with pronounced chemical exposure [3]. Steel corrosion initiates concrete cracking and spalling, and ultimately may cause structural failure, thus necessitating costly repairs, rehabilitation, and maintenance activities [4]. In response to these challenges, a growing demand for innovative and non-corrosive reinforcement alternatives has emerged to prolong service life and augment the sustainability of RC structures [5].

DOI: 10.21608/erj.2025.351884.1180
Received 10 January 2025; Received in revised form 17 February 2025; Accepted 03 March 2025
Available online 01 June 2025

Fiber-reinforced polymers (FRPs) present a viable alternative to conventional steel reinforcement, offering superior corrosion resistance, an enhanced strength-to-weight ratio, and electromagnetic transparency. These properties render FRP reinforcement particularly beneficial in environments susceptible to aggressive conditions, where steel corrosion is a concern, and in settings requiring electromagnetic compatibility, such as magnetic resonance imaging (MRI) facilities, where traditional steel reinforcement is typically unsuitable [1,6]. While the tensile characteristics of GFRP bars are well-established, their compressive behavior, particularly within RC columns, remains inadequately characterized, thereby highlighting a critical research gap with significant implications for structural design and material performance [3,4].

The pronounced disparity between the compressive and tensile capacities of GFRP reinforcement bars, with the latter exhibiting substantially reduced performance [2,7-9], constitutes a critical limitation. Consequently, prevailing design standards across jurisdictions, including the United States, Canada, and Italy, typically preclude the adoption of FRP bars as primary longitudinal reinforcement in RC columns. This constraint underscores the necessity for advanced investigations into the mechanical response of GFRP-reinforced concrete columns under eccentric loading, addressing pivotal gaps in knowledge to inform the development of robust and reliable design frameworks. This limitation underscores the critical need for continued exploration of the mechanical behavior of GFRP bars within RC columns, particularly under eccentric loading conditions. The present study addresses this research gap by evaluating the response of GFRP bars in RC columns under eccentric vertical loading, thereby contributing to the establishment of robust design methodologies for sustainable concrete infrastructure [6,10].

Extensive research has established that the confinement of concrete columns utilizing fiber-reinforced polymer materials significantly enhances their compressive strength and ductility under uniaxial loading conditions [2,5,11-6]. The efficacy of FRP confinement is governed by critical parameters, including the specific FRP type—such as carbon fiber-reinforced polymer (CFRP) or glass fiber-reinforced polymer (GFRP)—the number of FRP layers applied, and the transverse reinforcement spacing [4]. Notably, CFRP exhibits superior stiffness and strength augmentation, while GFRP is predominantly associated with enhanced ductility, reflecting the distinct mechanical properties of these composite materials [2]. Smaller spacing between ties or spirals increases concrete core confinement effectiveness and consequently improves the load-bearing capacity of the RC columns [2,4,11,17]. Additionally, the geometry of the transverse reinforcement plays a significant role in the stress distribution [18]. Circular-shaped ties, such as spirals or continuous hoops, provide a more uniform confinement pressure, and thus, are more efficient than rectangular or C-shaped ties [1].

The importance of proper material characterization and testing is also underlined by concerns surrounding size and slenderness effects on testing results. Existing experimental investigations have often been conducted using relatively small-scale specimens, which may conceal the possible influence of specimen size on the compressive strength [12]. The mechanical response of such specimens may be influenced by the boundary conditions imposed by the restraining effects of the end-bearing plates, which can alter the stress distribution and deformation characteristics during loading [2], and therefore results derived from small-scale specimens are less reliable and the models based on them may not be readily applicable to larger structures. Moreover, columns with larger slenderness ratios (length to diameter ratio) are more vulnerable to buckling failures and therefore require tailored reinforcement detailing compared with short columns [1,18]. Therefore, it is important to understand the impact of size and slenderness on the testing results, as these factors could have a considerable impact on the reliability of the research.

In light of the substantially lower compressive strength of GFRP bars, typically constituting 30% to 70% of their tensile capacity, prevailing design codes often discount the axial load contribution of longitudinal Glass Fiber-Reinforced Polymer (GFRP) reinforcement in concrete columns [2,4,5,19]. Experimental investigations reveal inconsistent strain compatibility among longitudinal FRP

reinforcement and surrounding concrete, necessitating its inclusion in analytical frameworks [3]. Given the comparable elastic modulus of FRP bars in compression and tension, predictive models must incorporate this property to accurately characterize their compressive behavior [3,19]. Thus, reliance on tensile parameters alone is inadequate, necessitating advanced constitutive models to account for the anisotropic and nonlinear response of GFRP reinforcement bars under compressive loads.

Finally, despite the numerous existing analytical models, no single model is universally accepted, and further research is essential to refine and develop more precise models for FRP confined columns [20,21]. Also, it is essential that all models should be validated using a comprehensive range of experimental results, particularly those generated from larger scale specimens considering different loading and confinement conditions.

1.1 Research Motivation and Niche Identification

While the structural behaviour of steel-RC columns under diverse loading regimes has been extensively studied, the response of GFRP-reinforced concrete columns, particularly under eccentric vertical loads, remains insufficiently characterized. Existing studies primarily address concentric axial loading, offering limited insight into the performance under eccentric loads, which more accurately represent in-situ conditions. Despite evidence suggesting that longitudinal GFRP reinforcement contributes to axial strength, current design standards neglect this owing to the significant disparity between the compressive and tensile characteristics of FRP bars together with the inappropriate reliance on tensile strength as a surrogate for compressive performance. Furthermore, the extrapolation of results from small-scale experimental studies to full-scale structural systems introduces additional uncertainties. Consequently, a critical research gap persists in assessing the efficacy of GFRP bars as a replacement for steel reinforcement bars in RC columns experiencing simultaneous axial and flexural demands. This study aims to bridge this gap by conducting a rigorous investigation into the behaviour of GFRP-reinforced columns under eccentric loading, encompassing various reinforcement configurations, to enhance predictive models and inform design standards.

1.2 Research significance

This study addresses critical challenges in structural engineering, focusing on the performance characteristics and durability of RC structures. Steel reinforcement, highly vulnerable to corrosion, remains a principal cause of RC degradation, accelerates structural failure and escalates maintenance costs. This research investigates the compressive characteristics of GFRP-RC columns subjected to eccentric loading, presenting a promising alternative to traditional steel reinforcement.

Characterized by exceptional corrosion resistance and a high strength-to-weight ratio, GFRP offers a solution to enhance the longevity of concrete structures while reducing long-term maintenance expenditures. However, the existing body of research predominantly explores concentric loading, leaving a substantial gap regarding GFRP's behavior under eccentric conditions that are critical for real-world applications.

This study bridges this gap by evaluating the load-bearing capacities and failure mechanisms of GFRP-reinforced columns under eccentric vertical loads. The outcomes are expected to influence design standards, fostering extended utilization of GFRP in corrosion-prone environments. Additionally, GFRP utilization can yield substantial economic and environmental benefits, such as reduced material consumption and minimized maintenance expenses. Eventually, this research contributes to a more nuanced understanding of GFRP-RC columns, driving the evolution of sustainable, cost-efficient infrastructure solutions.

2 Experimental program

2.1 Specimen Design and Fabrication

The study involved the design and fabrication of six RC column specimens to investigate their performance when subjected to eccentric vertically applied loading conditions. The specimens were categorized into two main groups: (1) Steel-RC Columns (Group A), which served as a benchmark for comparative analysis, and (2) GFRP-RC Columns (Group B) reinforced with glass fiber reinforced polymer bars, see Fig. 1. Each group comprised three specimens distinguished by varying eccentricity-to-depth ratios (e/t) while all parameters and values are explicitly listed in Table 1. All specimens possessed a rectangular cross-section with a constant width (b) of 250 mm and a total height of 1500 mm. With the aim to simulate a common loading condition for RC members in real world scenarios (i.e., an eccentric loading) and to avoid premature failure at column ends, haunches with a haunch depth (a) of 350 mm, 400 mm, and 450 mm were designed and incorporated at columns extremities with depths (t) of 250 mm (for specimens SA1 and SC1), 300 mm (for specimens SA2 and SC2), and 350 mm (for specimens SA3 and SC3), respectively.

Table 1. Geometric characteristics of the tested columns

Specimen ID		Column Dimensions					Geometric Properties	
		b (mm)	t (mm)	a (mm)	h (mm)	A (mm^2)	e (mm)	e/t (%)
Steel-RC	SA1	250	250	350	1500	62500	50	20
	SA2	250	300	400	1500	75000	50	17
	SA3	250	350	450	1500	87500	50	14
GFRP-RC	SC1	250	250	350	1500	62500	50	20
	SC2	250	300	400	1500	75000	50	17
	SC3	250	350	450	1500	87500	50	14

The Steel-RC column specimens (Group A) were reinforced with high-strength longitudinal/vertical steel bars (400 MPa yield strength). Specimen SA1 utilized four 12 mm diameter bars, achieving a reinforcement ratio of 0.72%. Specimen SA2 incorporated four 12 mm bars at the corners and two additional 10 mm bars along the compression and tension faces, yielding a 0.81% reinforcement ratio. Specimen SA3 employed six 12 mm bars, symmetrically distributed with three per face, resulting in a reinforcement ratio of 0.78%.

Conversely, the GFRP-RC specimens (Group B) were reinforced with 9.53 mm diameter vertical GFRP reinforcement bars (designated F3), coupled with transverse steel stirrups. Based on preliminary sizing, six No. 3 GFRP reinforcement bars were opted for Group B, resulting in a reinforcement ratio of 0.68% (0.25% steel-equivalent ratio, modulated via the $A_{s,E} = A_f \left(\frac{E_f}{E_s}\right)$ relationship) [7,22]. Reinforcement configurations varied across GFRP-RC columns. Specimen SC1 incorporated six No. 3 GFRP bars (three per side), SC2 featured an additional two No. 3 GFRP bars on the tension and compression sides, totaling eight bars with a reinforcement ratio of 0.76% (0.28% steel-equivalent ratio). SC3 included four additional No. 3 GFRP bars on the remaining sides, yielding ten GFRP bars at the perimeter and a reinforcement ratio of 0.82% (0.30% steel-equivalent ratio).

All specimens in both groups incorporated 8 mm diameter (T8) steel stirrups at 100 mm spacing, with three 8 mm diameter cap stirrups (3T8) at the column ends to mitigate stress concentrations and premature failure.

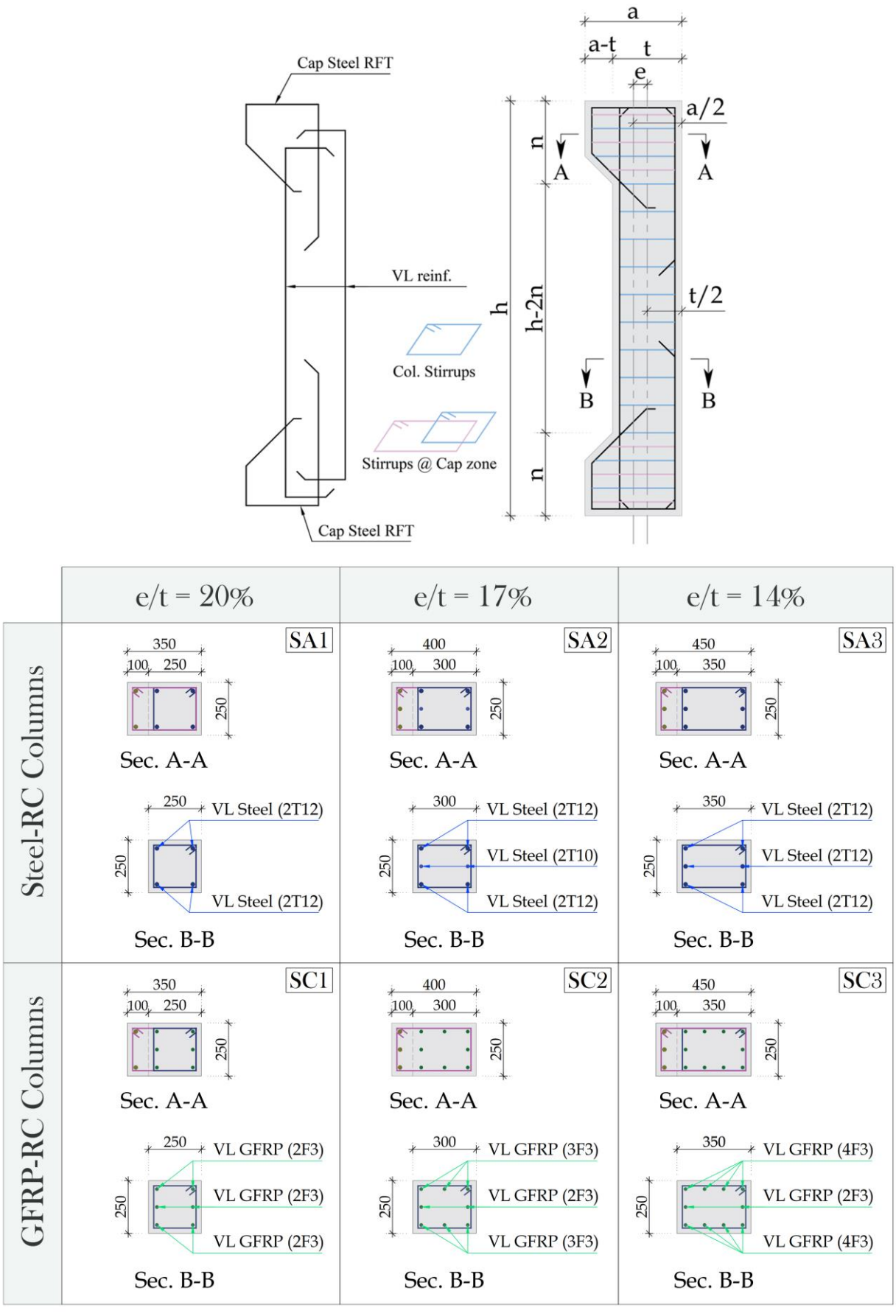

Fig. 1. Dimensions and reinforcement details of the RC columns (dimensions are in mm)

The transverse reinforcement exhibited 240 MPa yield strength, and all specimens maintained a clear concrete cover of 25 mm. Detailed specimen geometry and reinforcement layouts are outlined in Fig. 1, with reinforcement specifications highlighted in Table 2. An overview of the reinforcement cages, formwork, and cast specimens is demonstrated in Fig. 2.

2.2 Materials

Specimens were cast using ready-mixed normal-weight concrete, formulated to attain a target compressive strength of 30 MPa, achieving a mean compressive strength of 32.4 MPa. Longitudinal reinforcement was provided by Grade 60 steel bars, characterized by a yield strength of 400 MPa, an ultimate tensile strength of 600 MPa, and an elastic modulus of 200 GPa. Comparative analysis incorporated GFRP bars, featuring a tensile strength of 880 MPa and an elastic modulus of 53.4 GPa. Transverse reinforcement consisted of 8 mm steel ties, with a yield strength of 240 MPa and tensile strength of 360 MPa, and ultimate strain of 8.4%. Material properties are summarized in Table 3.

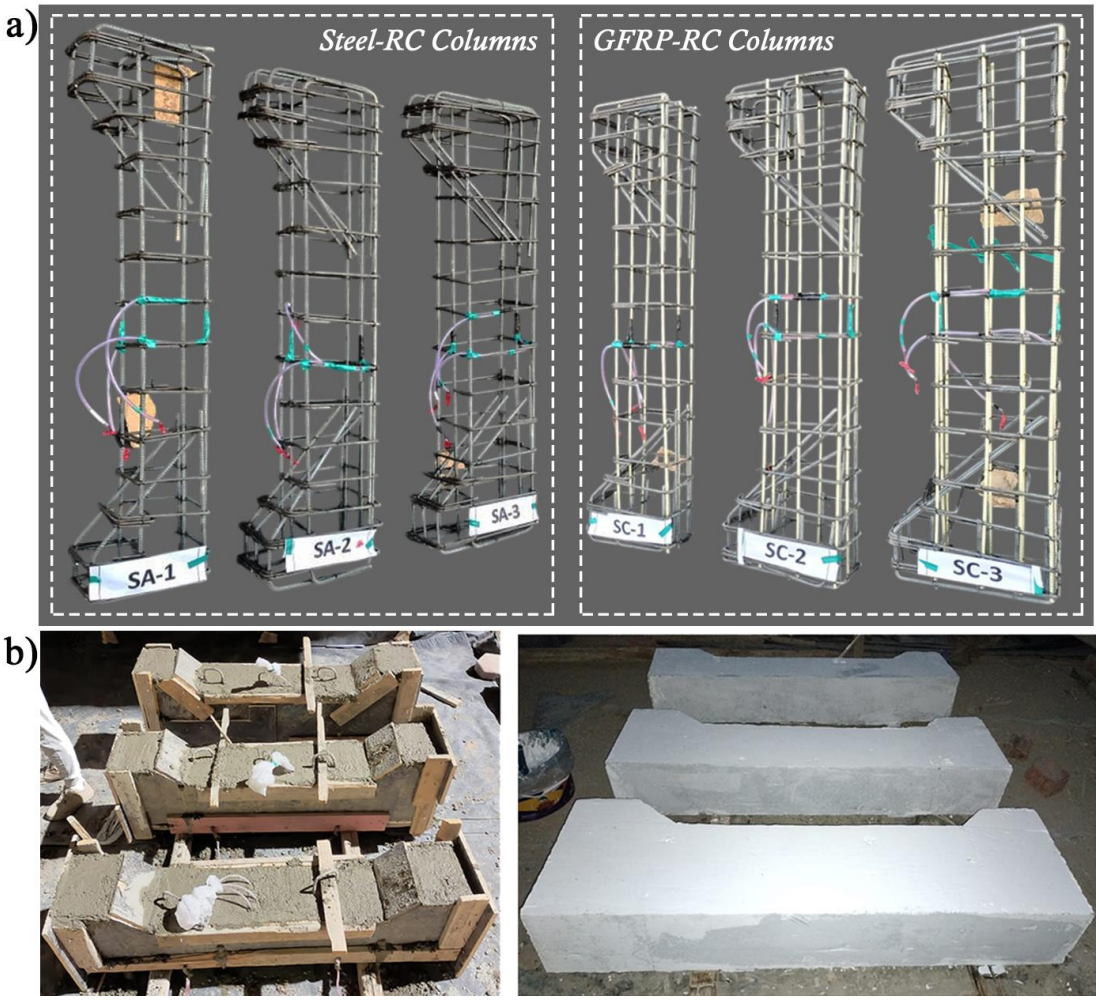

Fig. 2. Fabrication and preparation of the column specimens: a) overview of the assembled reinforcement cages, and b) wooden formwork and casted column specimens

2.3 Testing Setup and Procedure

The columns were vertically positioned and tested using a 5000 kN capacity servo-hydraulic machine, with pinned supports at both ends provided by rocker bearings. The loading system, modified with custom steel plates, rocker bearings, and a loading frame, applied eccentric loads of 50 mm at both ends to simulate realistic conditions (Fig. 3). Axial deformation was monitored via two LVDTs on opposing sides, while lateral displacement at mid-height was recorded using two additional horizontal LVDTs. Strain gauges on the vertical reinforcement and concrete at midsection captured axial and lateral strains on both tension and compression faces. Data acquisition was facilitated through a computer-based system interfacing with LVDTs and strain gauges for real-time measurement recording. The test configuration for eccentrically loaded columns is outlined in Fig. 3.

Table 2. Reinforcement details of the tested columns

Specimen ID		Vertical reinforcement					
		No. & size	A_s mm²	A_f mm²	$A_{s,E}$ mm²	ρ_V (%)	
						$\rho_{V-steel}$ (%)	ρ_{V-GFRP} (%)
Steel-RC	SA1	4T12[a]	452.39	-	-	0.72	-
	SA2	4T12 + 2T10[b]	609.47	-	-	0.81	-
	SA3	6T12	678.58	-	-	0.78	-
GFRP-RC	SC1	6F3	-	427.98	114.27	-	0.68
	SC2	8F3	-	570.64	152.36	-	0.76
	SC3	10F3	-	713.31	190.45	-	0.82

Table 3. Properties of steel and GFRP reinforcements

Bar type	Bar diameter (mm)	Cross-sections (mm2)	Yield strength (MPa)	Ultimate strength (MPa)	Modulus of elasticity (GPa)	Ultimate Strain (%)
Steel	12	113.1	400	600	200	5.7
	10	78.5	400			6.1
Steel ties	8	50.3	240	360		8.4
GFRP	9.53	71.3	-	880	53.4	2.0

3 Results and Discussion

A rigorous analysis was undertaken to explore the contribution of longitudinal reinforcement material and eccentric loading on the columns' mechanical behaviour. Axial load-displacement and strain profiles were generated to systematically assess the significance of these variables on column performance. The findings provide a comprehensive understanding of how reinforcement material and eccentricity modulate structural response, elucidating the columns' load-bearing capacities and failure mechanisms.

3.1 General Behavior and Failure Modes

The failure modes exhibited a progressive sequence, beginning with vertical hairline cracks at mid-height, which propagated into concrete spalling, core crushing, and culminated in longitudinal reinforcement buckling [1,10]. The progression of these events was contingent upon the type of vertical reinforcement and the applied eccentricity, as further discussed.

The steel-RC columns (Group A) exhibited brittle failure, marked by rapid concrete spalling and localized cracking, followed by buckling deformation of the longitudinal rebars, as depicted in Fig. 4. This failure mechanism reflects typical behavior in conventional RC columns, where insufficient confinement leads to premature steel yielding and compression failure of the concrete, culminating in reinforcement buckling [1,3]. Specimen SA1 (e/t = 20%) experienced an explosive failure, while SA2 and SA3 exhibited more gradual post-peak load reductions, indicating enhanced ductility. As eccentricity decreased (SA1 to SA3), load-displacement curves became progressively smoother, and failure modes transitioned toward greater ductility.

Conversely, those columns utilizing GFRP bars as reinforcement (Group B) demonstrated a more controlled, gradual failure, characterized by distributed cracking throughout the column height, with no explosive spalling at peak load, as visualized in Fig. 4. Despite concrete cover spalling, the concrete core remained largely intact in specimens SC2 and SC3, ascribed to the confinement offered by the transverse reinforcement. Notably, specimens tested under lower eccentricities exhibited a higher concentration of mid-height cracking, likely due to reduced lateral deflections and consequently diminished confinement.

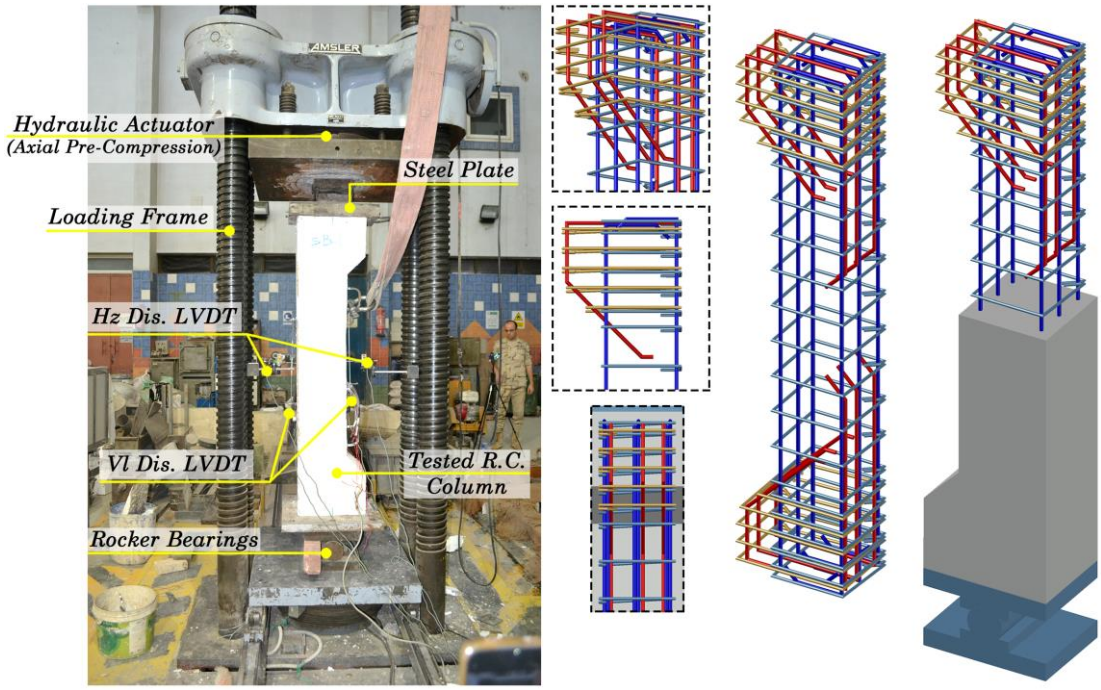

Fig. 3. Typical test setup and configuration for eccentrically loaded columns

As eccentricity decreased (from SC1 to SC3), a notable enhancement in specimen deformability was observed. Unlike the steel-RC columns, the vertical GFRP bars remained intact, with failure predominantly attributed to concrete crushing and GFRP buckling. This reduced brittleness, coupled with the absence of GFRP rupture, is a direct result of GFRP's exceptional tensile strength and ductility, along with the effective confinement from the steel stirrups [2,13]. These results underscore that, in

GFRP-RC columns with steel stirrups, failure mechanisms are dominated by concrete crushing and GFRP buckling, rather than GFRP rupture, even under eccentric loading conditions.

The detailed description of all the tested specimens is as follows:

- Specimens SA1, SC1 and SC3 had inclined compression cracks with localized concrete spalling at the mid-height of the compression-side of the columns.
- For specimens SA2 and SC2, cracks started at the column's ends, and subsequently propagated towards the column's mid-height. However, more extensive cracking was observed on the compression side, with the occurrence of wider cracks and more extensive cover spalling.
- For specimen SA3, multiple cracks with relatively uniform spacing were observed at the side of the specimen with higher lateral deflection (tension side), with some cracks propagating into the column's depth on the tension side.

Overall, the experimental findings demonstrate that with increasing eccentricity, cracking initiates at lower load levels, coupled with amplified vertical and lateral deflections. Moreover, the spalling progression in GFRP-RC columns was gradual, driven by the combined influence of transverse confinement and the elastic response of the GFRP longitudinal rebars.

Fig. 4. Failure modes of all tested columns

The results indicate that, while specimens in Groups A and B exhibited comparable initial responses, substantial divergences were observed in post-peak behavior and failure modes. Steel-RC columns experienced rapid failure, characterized by concrete cover spalling and buckling of the longitudinal rebars, whereas GFRP-RC columns demonstrated a more progressive failure, with widespread cracking along the column height. The failure mechanisms were further controlled by the eccentricity-to-depth ratio, with increasing eccentricity resulting in enhanced deformability across both reinforcement types.

3.2 Load-Displacement Behavior

The axial load-displacement curves for all tested specimens, shown in Fig. 5, exhibit a bilinear response characteristic of RC columns, with distinct phases. The initial quasi-linear phase corresponds to elastic behavior, while subsequent loading induces a loss of stiffness, transitioning into a non-linear regime and culminating in gradual load-carrying capacity degradation at peak load. A notable divergence between steel-RC and GFRP-RC columns arises in the post-peak behavior. GFRP-RC columns (Group A) exhibited an abrupt capacity drop post-peak, indicative of a brittle failure mechanism and concrete spalling. Conversely, Steel-RC columns (Group A) demonstrated a more progressive capacity reduction, accompanied by longitudinal bar buckling, reflecting enhanced plasticity and deformability

prior to failure [1,4]. The initial stiffness across all specimens was similar, independent of longitudinal rebars material, suggesting that the initial response is predominantly controlled by concrete elasticity rather than reinforcement type or configuration. These results corroborate similar findings in the literature [23]. Furthermore, steel-reinforced columns (Group A: SA1, SA2, SA3) presented a more pronounced peak load compared to GFRP-RC columns, with the latter exhibiting a sharp post-peak decline, while steel-RC columns demonstrated a more gradual load degradation.

Table 4 synthesizes the experimental data for all specimens, including ultimate load-carrying capacity (P_u), axial displacement at peak load (Δ_{peak}), maximum axial displacement (Δ_{max}), and normalized axial peak stress (f_{cc}/f_c'). The normalized axial peak stress (f_{cc}/f_c') for the columns ranged from 0.54 to 0.74. Steel-RC specimens exhibited values between 0.64 and 0.74, while GFRP-RC specimens ranged from 0.54 to 0.66. These results are congruent with the literature, which indicates an average compressive peak strength of 0.5 to 0.85 of the concrete's compressive strength [24,25]. The findings highlighted a clear decreasing trend of peak load in both Steel-RC and GFRP-RC columns coupled with the increase in load eccentricity [3]. Specimen SA1, which was tested under eccentricity to depth ratio (e/t) equal to 20%, exhibited a more ductile behaviour in comparison with specimens SA2 and SA3. This was the reference case with which other specimens were compared. Specimen SA3, tested under the lowest eccentric load ($e/t = 14\%$), exhibited a clearly defined peak load with an abrupt loss of capacity beyond this point, which suggests a more brittle failure. The abrupt decrease in the load carrying capacity can be rationalized by the occurred concrete spalling, leading to the subsequent buckling of the longitudinal steel reinforcement [6]. Nevertheless, Specimen SA2, which had an e/t ratio of 17%, exhibited similar general trends with specimen SA3 with a clear peak, and post peak behaviour with significantly less load-bearing capacity and deformability. Specimens SA1, SA2 and SA3 displayed a ductile behavior as a result of the participation of longitudinal steel reinforcement rebars in the deformation characteristics. De Luca et al. [1] reported similar trends in the performance of tested steel-RC columns.

Table 4. Summary of experimental results

Specimen ID		f_{cc}/f_c' (%)	$\varepsilon_{cc,peak}$ (με)	$\varepsilon_{cc,u}$ (με)	$\varepsilon_{cb,peak}$ (με)	$\varepsilon_{tb,peak}$ (με)	P_b (kN)	P_b/P_u (%)	μ_Δ	Δ_{peak}	Δ_{max}
Steel-RC	SA1	0.65	-2562	-8500	-3378	258	164.50	13.60	1.34	6.65	9.47
	SA2	0.70	-2400	-8030	-2689	272	180.49	11.50	1.18	5.99	11.89
	SA3	0.74	-2640	-8308	-2326	358	182.14	9.33	1.14	5.93	13.66
GFRP-RC	SC1	0.54	-2318	-10700	-2571	1287	61.09	6.08	1.26	4.01	5.46
	SC2	0.59	-2948	-8310	-2289	916	67.66	5.12	1.14	4.31	5.03
	SC3	0.66	-1738	-10732	-1535	143	44.30	2.56	1.13	4.90	6.83

For Group B (GFRP-RC columns), the axial load-displacement curves exhibited similar initial elastic response as Group A. Specimen SC1, with an eccentricity-to-depth ratio equal to 20%, showed a relatively rapid increase in load up to its peak load, while beyond this point a significant drop in the load-bearing capacity occurred after a limited post-peak response. Meanwhile, specimen SC2, which had an eccentricity-to-depth ratio of 17%, exhibited a similar trend, with a less pronounced post-peak strength degradation than specimens SC1, which may be a consequence of the increased concrete core volume due to larger depth d. However, its maximum deformation value was lesser than the achieved value from specimen SC1. The behaviour of specimen SC3 ($e/t = 14\%$) differs from specimens SC1

and SC2 with the specimen sustaining a higher peak load, however, exhibiting a pronounced lowered strength and more brittle behaviour.

Overall, the maximum load of all specimens exhibits a decrement as the eccentricity of the applied load increases. Post-peak behaviour of eccentrically loaded columns with high e/t ratios (Groups A and B) is marked by a more progressive strength degradation, as opposed to the abrupt failure observed in low e/t ratio specimens. This is a consequence of tensile forces developed at the column cross-section under greater eccentric loading [26,27], consistent with the anticipated ductile failure mechanism when bending dominates. Subsequent to peak load, the tensile zone undergoes significant strain, potentially triggering reinforcement yielding and a more incremental progression of damage. Among specimens with comparable eccentricity ratios, steel-RC specimens consistently demonstrated superior load-bearing capacity relative to GFRP-RC counterparts. Furthermore, while peak load capacity decreases with increasing eccentricity, the maximum axial displacement (Δ_{max}) generally increases with elevated eccentricity.

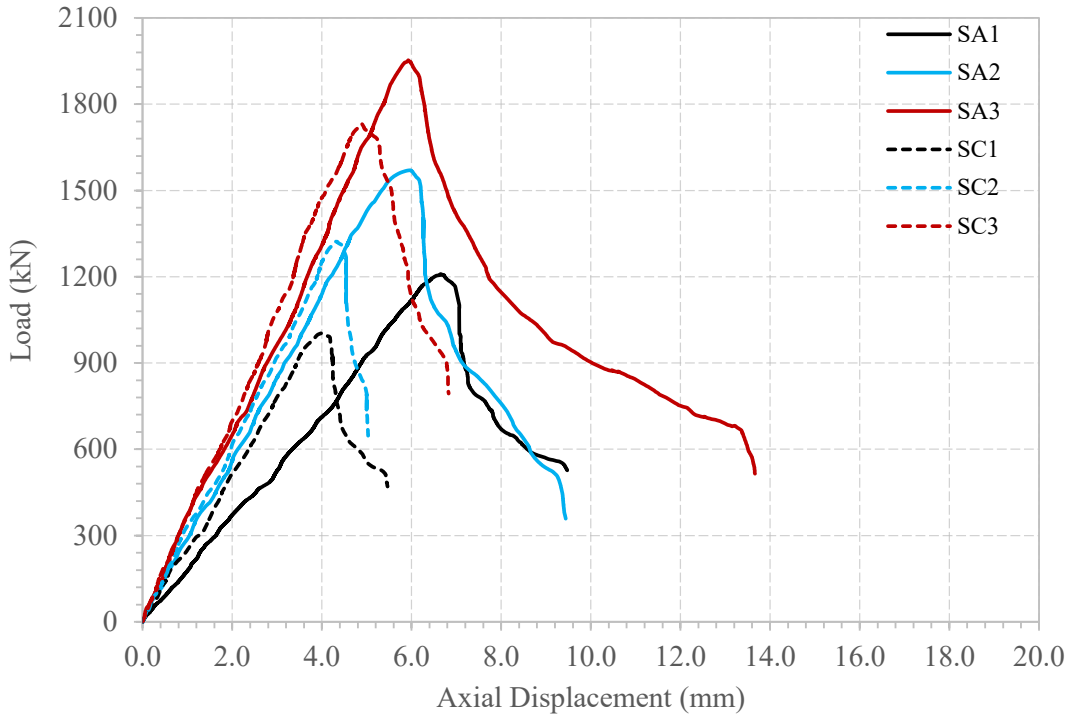

Fig. 5. Load versus axial displacement

3.3 Strength and Deformation Capacity

The interaction between the applied axial load versus the resulting concrete strain on the compression side of each column is demonstrated in Fig. 6. Three distinct phases of behavior were identified, in line with the different stages of concrete response under eccentric compression. Initially, the curves demonstrate linearity, representing the elastic pre-crack range where strains increase proportionally with the exerted load. The inflection point, where the stress-strain curve deviates from linearity, signifies the onset of stiffness degradation. The second phase, a non-linear transition, involves concrete expansion and strain amplification, leading to the formation of microcracks. In the third phase, post-peak, the concrete experiences extensive expansion and crushing due to significant microcracking [26]. Maximum compressive strains reached up to $-10700\ \mu\varepsilon$, while peak load was attained at substantially

lower strains, ranging from -1738 to -2948 $\mu\varepsilon$. This suggests considerable post-peak displacements, particularly in GFRP-RC specimens.

Table 4 summarizes the experimental findings, including peak loads (P_u) and their associated axial displacements (Δ_{peak}), concrete strain on the compression side ($\varepsilon_{cc,peak}$), and strains in the vertical reinforcement at peak load ($\varepsilon_{cb,peak}$ for compression and $\varepsilon_{tb,peak}$ for tension). Strain measurements at mid-height of the columns reveal differential strain responses in the reinforcement, with tension-side bars experiencing tensile strain and compression-side bars exhibiting compressive strain, reflective of the structural response under load. The reinforcement's contribution to the ultimate load (P_b/P_u) is quantified through an analytical approach that integrates axial strain, elastic modulus, and cross-sectional area, under the assumptions of linear elastic behavior and uniform strain distribution, aligning with the principles of superposition and material linearity.

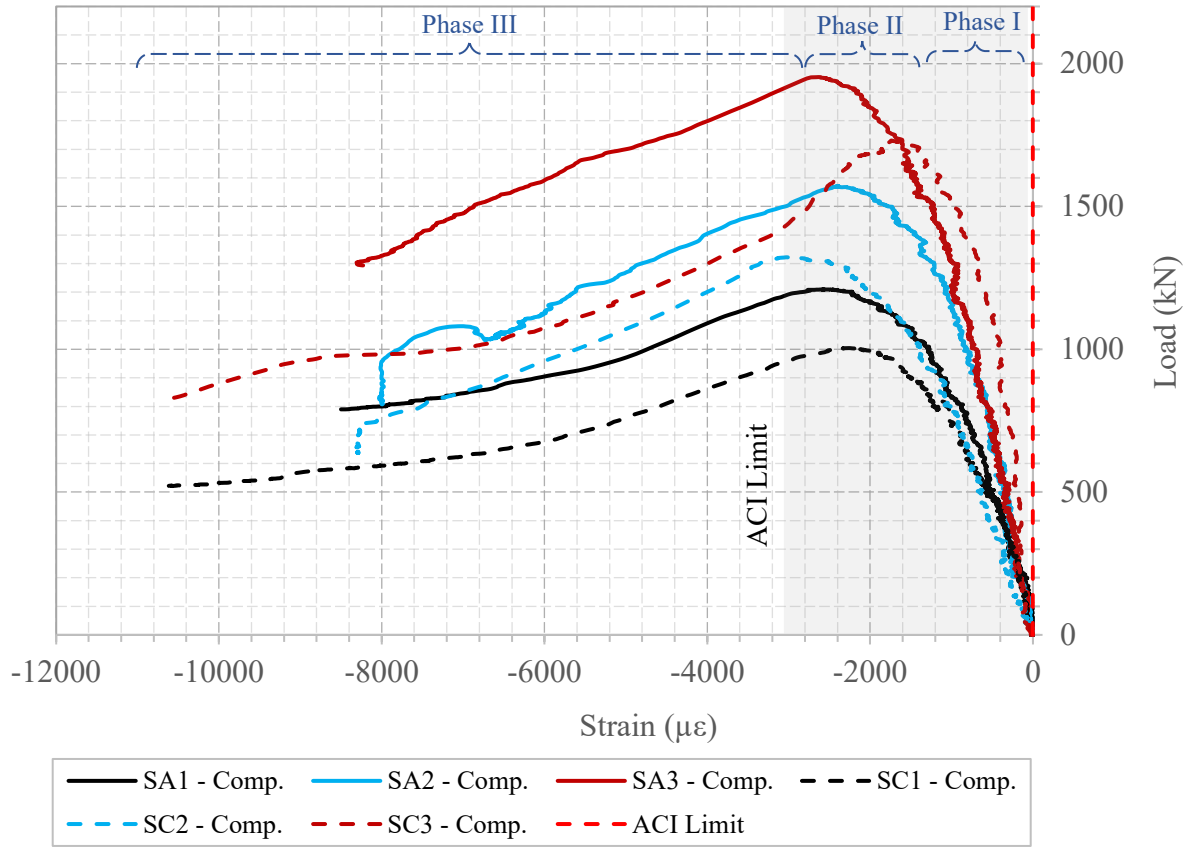

Fig. 6. Load versus concrete strain on compression side

The comparatively limited contribution of GFRP reinforcement to the maximum load-bearing capacity, ranging from 2.9% to 4.5%, underscores its limited influence relative to steel reinforcement, which contributed approximately 11.6%. This disparity is predominantly attributable to the significantly lower elastic modulus of GFRP, thereby highlighting the preeminent role of the concrete matrix's axial stiffness in load-bearing capacity. Conversely, the mechanical properties of the longitudinal reinforcement predominantly influence post-peak ductility and structural resilience.

Steel-RC columns (Group A) demonstrated superior peak load capacities and post-peak stiffness compared to GFRP-RC columns (Group B). Notably, specimen SA1 exhibited higher ductility than SA2 and SA3, which showed reduced ductile behavior. Steel-RC columns displayed pronounced stiffness degradation and strength reduction post-peak, indicative of brittle failure under minimal eccentric

loading. Steel-RC columns achieved higher peak strains ($\varepsilon_{cb,peak}$ and $\varepsilon_{tb,peak}$) than their GFRP counterparts, with GFRP bars reaching maximum strain at lower load levels, as a result of the substantially lower elastic modulus of GFRP [4,22]. This disparity underscores that, under eccentric loading conditions, steel reinforcement achieves higher stress levels at peak load compared to GFRP reinforcement, further emphasizing the influence of material properties on structural performance.

The stress-strain response of GFRP-RC columns was strongly influenced by load eccentricity. Specimens subjected to higher eccentricities (SC1 and SC2) exhibited similar stress-strain responses, characterized by a rapid post-peak load loss and marginal increases in peak concrete strain. In contrast, specimen SC3, subjected to lower eccentricity, displayed a more ductile response with higher compressive strains and a more pronounced plastic region, suggesting that reduced eccentricity enhances the ductility of GFRP-RC columns through extended plastic deformation and controlled strength degradation [3].

Group B specimens exhibited similar ascending phases of the axial load-compressive strain curve, dominated by linear behavior. However, specimen SC3 exhibited a more ductile response, with a gradual post-peak load reduction, indicating more stable crack progression in columns with lower e/t ratios and better post-peak response relative to other specimens in this group.

3.4 Ductility

Ductility, identified to as the capacity of a structural element to sustain substantial inelastic deformation prior to failure, was quantified through the displacement ductility index (μ_Δ), which is expressed as the ratio of axial displacement at ultimate failure (Δ_u) to the displacement at the initiation of concrete crushing (Δ_y). This approach was specifically employed to mitigate subjectivity in the identification of yield points for GFRP-RC columns, while maintaining methodological consistency with conventional steel-reinforced concrete structures [11,12,15,22]. The deformation response of GFRP-RC columns was assessed adopting the established framework for steel-RC columns [28], ensuring a comprehensive assessment of plasticity, including the characterization of strain-softening failure modes. The experimentally derived ductility indices are listed in Table 4.

The results demonstrate a substantial impact of reinforcement material properties and configuration on ductility. Steel-RC specimens (Group A) exhibited significantly enhanced ductility, attributable to the yielding characteristics of steel-reinforcement, which enables a progressive failure mode by sustaining stress at elevated strain levels. Whereas, the linear-elastic behavior of GFRP reinforcement severely limits plastic deformation, resulting in diminished ductility. Furthermore, a heighten eccentricity-to-depth ratio (e/t) from 14% to 20% led to a marked improvement in ductility for both reinforcement types. This enhancement is credited to the predominance of flexural mechanisms under eccentric loading conditions, where initial flexural-tension cracking transitions to compression-dominated failure, facilitating the propagation of cracks and the activation of transverse reinforcement. This interaction mitigates the abrupt failure typically observed in short columns, underlining the pivotal role of reinforcement properties and loading configurations in governing post-peak response and collapse mechanisms in RC columns.

4 Conclusions

This experimental investigation evaluated the axial load-displacement response of RC columns subjected to eccentric loading, with a focus on the comparative performance of longitudinal steel and GFRP reinforcement in conjunction with transverse steel stirrups. The following conclusions are drawn:

- GFRP-reinforced concrete (GFRP-RC) columns exhibited comparable ultimate load capacities to steel-reinforced concrete (steel-RC) columns under eccentric loading. However, the normalized

ultimate axial stress for GFRP-RC specimens ranged from 54% to 66% of the average concrete compressive strength, marginally lower than the 64% to 74% observed for steel-RC specimens.

- Distinct failure mechanisms were identified: steel-RC columns exhibited brittle failure characterized by sudden concrete cover spalling and subsequent buckling of longitudinal rebars, whereas GFRP-RC columns demonstrated a more progressive failure mode with distributed cracking.
- Ductility, quantified via the displacement ductility index (μ_Δ), was significantly influenced by reinforcement material and eccentricity. Steel-RC columns exhibited superior ductility due to the yielding behavior of steel reinforcement, which facilitated sustained stress at high strains. Increasing the eccentricity ratio (e/t) enhanced ductility for both reinforcement types, with higher eccentricities promoting greater deformation capacity through flexural mechanisms.
- The GFRP reinforcement exhibited a peak axial load contribution ranging from 2.9% to 6.08%, markedly inferior to the 9.33% to 13.6% provided by steel reinforcement. This disparity can be linked to the comparatively lower elasticity and compressive resistance of GFRP, emphasizing the dominant role of concrete axial stiffness in the initial loading phase.
- Loading eccentricity exerted a considerable effect on structural behavior. A decrease in the e/t ratio reduced brittleness and enhanced ductility, while increasing the e/t ratio diminished load-carrying capacity for both GFRP-RC and steel-RC columns. The activation of transverse reinforcement under higher eccentricities delayed concrete core crushing, mitigating abrupt failure.

References

1. De Luca, F. Matta, and A. Nanni, “Behavior of Full-Scale Glass Fiber-Reinforced Polymer Reinforced Concrete Columns under Axial Load,” ACI Struct. J., vol. 107, no. 5, pp. 589–596, 2010, doi: 10.14359/51663912.
2. M. Thériault, K. W. Neale, and S. Claude, “Fiber-Reinforced Polymer-Confined Circular Concrete Columns: Investigation of Size and Slenderness Effects,” J. Compos. Constr., vol. 8, no. 4, pp. 323–331, Aug. 2004, doi: 10.1061/(ASCE)1090-0268(2004)8:4(323).
3. H. A. Hasan, M. N. Sheikh, and M. N. S. Hadi, “Maximum axial load carrying capacity of Fibre Reinforced-Polymer (FRP) bar reinforced concrete columns under axial compression,” Structures, vol. 19, pp. 227–233, Jun. 2019, doi: 10.1016/j.istruc.2018.12.012.
4. F. Abed, A. El Refai, and N. ElMesalami, “Compressive Behaviour of Glass Fiber-Reinforced Polymer (GFRP) Reinforced Concrete Columns,” in 10th International Conference on FRP Composites in Civil Engineering, vol. 198, A. Ilki, M. Ispir, and P. Inci, Eds., in Lecture Notes in Civil Engineering, vol. 198. , Cham: Springer International Publishing, 2022, pp. 851–858. doi: 10.1007/978-3-030-88166-5_73.
5. N. Elmessalami, A. El Refai, and F. Abed, “Fiber-reinforced polymers bars for compression reinforcement: A promising alternative to steel bars,” Constr. Build. Mater., vol. 209, pp. 725–737, Jun. 2019, doi: 10.1016/j.conbuildmat.2019.03.105.
6. De Luca, F. Matta, and A. Nanni, “Behavior of Full-Scale Concrete Columns Internally Reinforced with Glass FRP Bars under Pure Axial Load,” Compos. Polycon, pp. 1–10, 2009.
7. H. el-Kady, O. Amer, A. H. Ali, and H. Haggag, “Experimental Investigation on the Cyclic In-Plane Behavior of GFRP-Reinforced Concrete Shear Walls,” Buildings, vol. 12, no. 11, Art. no. 11, Nov. 2022, doi: 10.3390/buildings12111948.
8. H. el-Kady, O. Amer, A. H. Ali, and H. Haggag, “Hysteretic performance of hybrid GFRP-steel reinforced concrete shear walls: An experimental Investigation,” J. Cem. Based Compos., vol. 4, no. 3, p. 5736, 2022, doi: 10.36937/cebacom.2022.5736.
9. H. el-Kady, O. Amer, A. Shawky, and H. Haggag, “Quasi-static Cyclic In-plane Testing of Slender GFRP-Reinforced Concrete Shear Walls,” Civ. Eng. Limits, vol. 3, no. 3, p. 1737, 2022, doi: 10.36937/cebel.2022.1737.

10. H. Tobbi, A. S. Farghaly, and B. Benmokrane, "Concrete Columns Reinforced Longitudinally and Transversally with Glass Fiber-Reinforced Polymer Bars," ACI Struct. J., vol. 109, no. 4, pp. 551–558, 2012, doi: 10.14359/51683874.
11. M. Z. Afifi, H. M. Mohamed, and B. Benmokrane, "Axial Capacity of Circular Concrete Columns Reinforced with GFRP Bars and Spirals," J. Compos. Constr., vol. 18, no. 1, p. 04013017, 2013, doi: 10.1061/(ASCE)CC.1943-5614.0000438.
12. M. Z. Afifi, H. M. Mohamed, and B. Benmokrane, "Strength and Axial Behavior of Circular Concrete Columns Reinforced with CFRP Bars and Spirals," J. Compos. Constr., vol. 18, no. 2, p. 04013035, 2013, doi: 10.1061/(ASCE)CC.1943-5614.0000430.
13. N. ElMessalami, F. Abed, and A. El Refai, "Response of concrete columns reinforced with longitudinal and transverse BFRP bars under concentric and eccentric loading," Compos. Struct., vol. 255, p. 113057, Jan. 2021, doi: 10.1016/j.compstruct.2020.113057.
14. Hadhood, H. M. Mohamed, and B. Benmokrane, "Failure Envelope of Circular Concrete Columns Reinforced with GFRP Bars and Spirals," ACI Struct. J., vol. 114, no. 6, Nov. 2017, doi: 10.14359/51689498.
15. H. M. Mohamed, M. Z. Afifi, and B. Benmokrane, "Performance Evaluation of Concrete Columns Reinforced Longitudinally with FRP Bars and Confined with FRP Hoops and Spirals under Axial Load," J. Bridge Eng., vol. 19, no. 7, p. 04014020, Jul. 2014, doi: 10.1061/(ASCE)BE.1943-5592.0000590.
16. Y.-Y. Ye, Y. Zhuge, S. T. Smith, J.-J. Zeng, and Y.-L. Bai, "Behavior of GFRP-RC columns under axial compression: Assessment of existing models and a new axial load-strain model," J. Build. Eng., vol. 47, p. 103782, Apr. 2022, doi: 10.1016/j.jobe.2021.103782.
17. H. Karim, M. N. Sheikh, and M. N. S. Hadi, "Axial load-axial deformation behaviour of circular concrete columns reinforced with GFRP bars and helices," Constr. Build. Mater., vol. 112, pp. 1147–1157, Jun. 2016, doi: 10.1016/j.conbuildmat.2016.02.219.
18. Y.-L. Bai, J.-G. Dai, and J. G. Teng, "Buckling of steel reinforcing bars in FRP-confined RC columns: An experimental study," Constr. Build. Mater., vol. 140, pp. 403–415, Jun. 2017, doi: 10.1016/j.conbuildmat.2017.02.149.
19. H. A. Hasan, H. Karim, H. A. Goaiz, A. M. Cabe, M. N. Sheikh, and M. N. S. Hadi, "Performance evaluation of normal- and high-strength concrete column specimens reinforced longitudinally with different ratios of GFRP bars," Structures, vol. 47, pp. 1428–1440, Jan. 2023, doi: 10.1016/j.istruc.2022.11.056.
20. M. Z. Afifi, H. M. Mohamed, and B. Benmokrane, "Theoretical stress–strain model for circular concrete columns confined by GFRP spirals and hoops," Eng. Struct., vol. 102, pp. 202–213, Nov. 2015, doi: 10.1016/j.engstruct.2015.08.020.
21. H. J. Zadeh and A. Nanni, "Design of RC Columns Using Glass FRP Reinforcement," J. Compos. Constr., vol. 17, no. 3, pp. 294–304, Jun. 2013, doi: 10.1061/(ASCE)CC.1943-5614.0000354.
22. M. Saad, O. Amer, Hesham, Haggag, and A. H. Ali, "Experimental Investigation of the In-Plane Cyclic Behavior of Hybrid GFRP-Steel Reinforced Squat Shear Walls," Eng. Res. J., 2025.
23. Mirmiran and M. Shahawy, "Behavior of Concrete Columns Confined by Fiber Composites," J. Struct. Eng., vol. 123, no. 5, pp. 583–590, May 1997, doi: 10.1061/(ASCE)0733-9445(1997)123:5(583).
24. M. Elchalakani, A. Karrech, M. Dong, M. S. Mohamed Ali, and B. Yang, "Experiments and Finite Element Analysis of GFRP Reinforced Geopolymer Concrete Rectangular Columns Subjected to Concentric and Eccentric Axial Loading," Structures, vol. 14, pp. 273–289, Jun. 2018, doi: 10.1016/j.istruc.2018.04.001.
25. N. Mohamed, A. S. Farghaly, B. Benmokrane, and K. W. Neale, "Drift Capacity Design of Shear Walls Reinforced with Glass Fiber-Reinforced Polymer Bars," ACI Struct. J., vol. 111, no. 6, Nov. 2014, doi: 10.14359/51687099.
26. L. Sun, M. Wei, and N. Zhang, "Experimental study on the behavior of GFRP reinforced concrete columns under eccentric axial load," Constr. Build. Mater., vol. 152, pp. 214–225, Oct. 2017, doi: 10.1016/j.conbuildmat.2017.06.159.
27. J. Youssef and M. N. S. Hadi, "Axial load-bending moment diagrams of GFRP reinforced columns and GFRP encased square columns," Constr. Build. Mater., vol. 135, pp. 550–564, Mar. 2017, doi: 10.1016/j.conbuildmat.2016.12.125.
28. S. Pessiki and A. Pieroni, "Axial Load Behavior of LargeScale Spirally Reinforced HighStrength Concrete Columns," ACI Struct. J., vol. 94, no. 3, pp. 304–314, 1997, doi: 10.14359/482.